JMEPEG (2004) 13:504-508
DOI: 10.1361/10599490419171

1059-9495/$19.00

The Effect of Si Addition on Crystallization Behavior of Amorphous Al-Y-Ni Alloy

M. Gögebakan

(Submitted October 24, 2003)

This article reports the effect of silicon (Si) addition upon the crystallization behavior and mechanical properties of an amorphous AlYNi alloy. An amount of 1 at.% Si was added to a base alloy of $Al_{85}Y_5Ni_{10}$ either by substitution for yttrium (Y) to form $Al_{85}Y_4Ni_{10}Si_1$, or by substitution for nickel (Ni) to form $Al_{85}Y_5Ni_9Si_1$. Differential scanning calorimetry (DSC) of all three alloys showed three exothermic peaks. Comparing the peak temperature for the first exothermic peak, a significant shift occurs toward the lower temperature. This indicates that 1 at.% substitutions of Y or Ni by Si decreases the stability of the amorphous phase. DSC study of these amorphous alloys during isothermal annealing at temperatures about 5-15 K lower than their first crystallization peaks showed that the formation of α-Al nanocrystals via primary crystallization occurred without an incubation period. The Avrami time exponent (n) of the primary crystallization from the amorphous structure was determined to be 1.00-1.16 using the Johnson-Mehl-Avrami (JMA) analysis. This suggested a diffusion-controlled growth without nucleation. However, a DSC study of these amorphous alloys during isothermal annealing at higher temperatures between 585 and 605 K showed a clear incubation period during the formation of the Al_3Ni and Al_3Y intermetallic phases. An *n* value of 3.00-3.45 was determined using JMA analysis. This suggested that the transformation reaction involved a decreasing nucleation rate and interface-controlled growth behavior. The tensile strength σ_f and Vickers hardness for these amorphous alloys are in the range 1050-1250 MPa and 380-398 diamond pyramid hardness number (1 diamond pyramid hardness number = 1 kg/mm^2 = 9.8 MPa), respectively.

Keywords AlYNiSi alloy, amorphous, crystallization, differential scanning calorimetry, mechanical properties, x-ray diffractometry

1. Introduction

Aluminum (Al)-based amorphous alloys manufactured by rapid solidification, particularly those containing rare earths and transition metals, have attracted much attention due to their remarkable mechanical properties such as high tensile strength, hardness, and good ductility.[1,2] Furthermore, partial crystallization of the Al-based amorphous alloys has led to the formation of a composite microstructure of nanocrystalline α-Al particles dispersed in an amorphous matrix. Such a composite microstructure exhibits ultra high tensile mechanical properties compared with either its fully amorphous or crystalline counterparts. The study of these alloys with high mechanical strength and good ductility, even in a coexistent state of amorphous and crystalline phase, is therefore important for the future development of the light and strong materials. Although the effects of Cu,[4] Co,[5,6] Sr,[7] Fe, or Mn[8] additions on crystallization behavior or microstructure of rapidly solidified AlYNi alloys have been investigated, the effect of Si addition has not been investigated in detail.

The density of silicon (Si) is 2.3 kg cm^{-3}, and that of Al is 2.7 kg cm^{-3}, so Si is one of the few elements that may be added to Al without an increase in density. In applications in which Al-based alloys are used, low density is often more important than high strength. Thus, the general density of AlYNi amorphous alloys can be reduced by additions of Si for Y and Ni.

In the present investigation, the effect of Si addition on the crystallization behavior and mechanical properties of an amorphous $Al_{85}Y_5Ni_{10}$ alloy has been investigated by substituting 1 at.% Si for yttrium (Y) and nickel (Ni), and using a combination of differential scanning calorimetry (DSC) and x-ray diffraction (XRD) to investigate the resulting effects.

2. Experimental

Amorphous $Al_{85}Y_5Ni_{10}$, $Al_{85}Y_4Ni_{10}Si_1$, and $Al_{85}Y_5Ni_9Si_1$ alloy ribbons were manufactured from a mixture of pure Al (99.99%), Ni (99.95%), Y (99.9%), and Si (99.99%) by melt spinning with a wheel surface velocity of 45 ms under Ar atmosphere. The compositions are given in nominal at.%. The resulting melt-spun ribbons were typically 30 μm in thickness and 3 mm in width. The crystallization behavior of the as-melt-spun ribbons were studied by DSC (using a TA2200 thermal analyzer with TA2010 DSC cell) using a combination of continuous heating from 350-750 K at a constant heating rate of 20 K min^{-1} and isothermal annealing at different temperatures. The structures of the as-melt-spun and annealed ribbons were examined by XRD (PW 1729 diffractometer with filtered Cu-Kα, Philips, Amsterdam, The Netherlands). The microhardness and tensile strength of the ribbons were measured using a Vickers microhardness tester at a 50 g load and Instron-type tensile testing machine at a strain rate of 8.3×10^{-4} s^{-1}. Ten symmetrical indentations and five tensiles were used to determine the average microhardness value and tensile fracture strength.

M. Gögebakan, Department of Physics, Faculty of Art and Science, Kahramanmaras Sutcu Imam University, Kahramanmaras 46100, Turkey. Contact e-mail: gogebakan@hotmail.com.

3. Results and Discussion

Figure 1 shows typical XRD spectra of the as-melt-spun $Al_{85}Y_5Ni_{10}$, $Al_{85}Y_4Ni_{10}Si_1$, and $Al_{85}Y_5Ni_9Si_1$ alloys produced in the same conditions. The XRD spectra of all three alloys consisted of a broad diffraction peak ($2\Theta \approx 38°$) with an additional smaller overlapping broad peak at a higher angle ($2\Theta \approx 44°$), which is typical of an amorphous Al alloy with a low concentration of rare earth elements. The smaller overlapping broad peak is very close to the expected position of the {200} Al peak, and the Scherrer equation[9] was used to interpret this peak as being due to very small crystalline Al particles of about 3 nm in size. Therefore, this observation indicates the presence of a crystalline fraction inside the amorphous matrix.

Figure 2 shows typical DSC traces obtained from the as-melt-spun $Al_{85}Y_5Ni_{10}$, $Al_{85}Y_4Ni_{10}Si_1$, and $Al_{85}Y_5Ni_9Si_1$ alloys using continuous heating at 20 K min^{-1}. The data for different compositions are shifted vertically to avoid overlap. Each DSC trace consisted of three exothermic peaks. $Al_{85}Y_5Ni_{10}$ exhibited a broad exothermic peak at about 500 K, and second and third exothermic peaks at 610 and 640 K, respectively. $Al_{85}Y_4Ni_{10}Si_1$ exhibited a first exothermic peak at 473 K followed by two exothermic peaks at 620 and 660 K. $Al_{85}Y_5Ni_9Si_1$ exhibited a small broad exothermic peak at 470 K, followed by peaks at 620 and 700 K. Comparing the peak temperature for the first exothermic peaks, a significant shift occurred toward a lower temperature with the addition of 1 at.% Si. This indicates that 1 at.% substitutions of Si for Y or Ni decreases the stability of the amorphous phase. In general, fully amorphous alloys exhibit a clear glass-transition temperature prior to the first crystallization peak, however, it is well-known that amorphous Al alloys with low solute contents do not exhibit a glass-transition temperature. In these alloys, primary crystallization occurs at pre-existing nuclei.[10]

Two temperatures close to the first and second exothermic reactions were chosen for subsequent isothermal heating DSC studies. Figure 3 shows typical calorimetry traces of the amorphous $Al_{85}Y_5Ni_{10}$, $Al_{85}Y_4Ni_{10}Si_1$, and $Al_{85}Y_5Ni_9Si_1$ alloys obtained from isothermal annealing at temperatures about 5-15 K lower than their first crystallization peak. As seen in Fig. 3, isothermal annealing calorimetry traces of the first exothermic reaction showed that the reaction occurred with no incubation period. Isothermal calorimetry curves without an incubation stage have been observed previously for AlNiCe[11] and AlNiY[12] ternary alloy systems. This absence of an incubation stage was interpreted as an indication that the reaction occurs entirely by thermally activated growth from pre-existing nuclei in the amorphous phase. Therefore, the absence of an incubation period in the $Al_{85}Y_5Ni_{10}$, $Al_{85}Y_4Ni_{10}Si_1$, and $Al_{85}Y_5Ni_9Si_1$ alloys indicates that the transformation probably occurs through a growth process without nucleation.

Using the data obtained from the isothermal calorimetry experiments, the transformation kinetics can be analyzed using the Johnson-Mehl-Avrami (JMA) equation[13]:

$$X = 1 - \exp(-Kt^n)$$

where X is the volume fraction crystallized in time t, n is the Avrami time exponent that indicates the nature of the reaction and has a value related to the nucleation and growth behavior during transformation, and K is the kinetic coefficient. The Avrami exponent n is obtained from plots of $\ln[-\ln(1 - X)]$ versus $\ln(t)$. For the first stage of crystallization, JMA analysis gave a low value of the Avrami time exponent (i.e., in the range of 1.00-1.16). These values indicate that the reaction occurred by diffusion-controlled growth of the α-Al nanocrystals. Given that the particles are approximately spherical, the particle radius in one dimension increases according to $D \propto t^{0.35}$. Simple diffusion-controlled growth is usually proportionally to $t^{0.5}$.

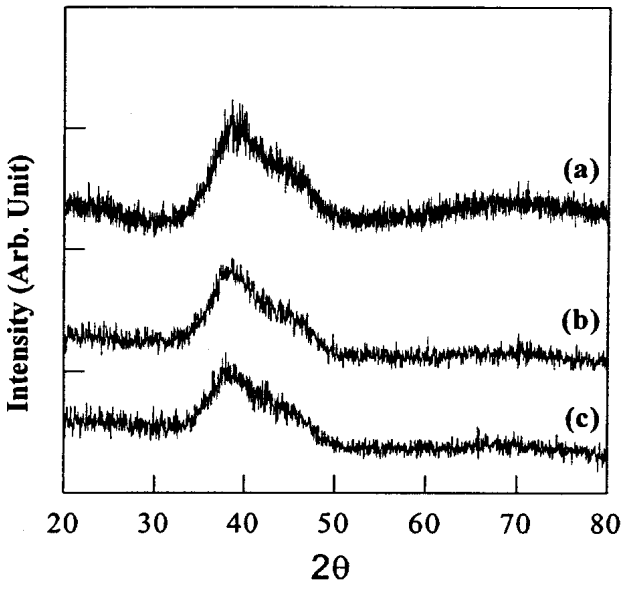

Fig. 1 XRD spectra from the as-melt-spun (**a**) $Al_{85}Y_5Ni_{10}$, (**b**) $Al_{85}Y_4Ni_{10}Si_1$, and (**c**) $Al_{85}Y_5Ni_9Si_1$ alloys

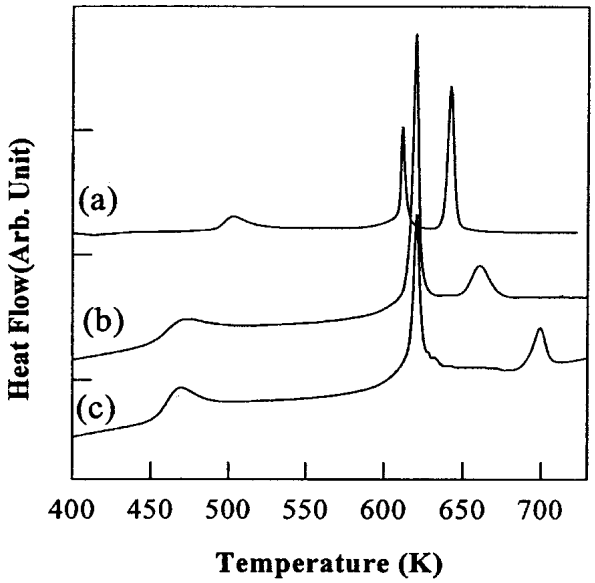

Fig. 2 DSC traces obtained from as-melt-spun (**a**) $Al_{85}Y_5Ni_{10}$, (**b**) $Al_{85}Y_4Ni_{10}Si_1$, and (**c**) $Al_{85}Y_5Ni_9Si_1$ alloys

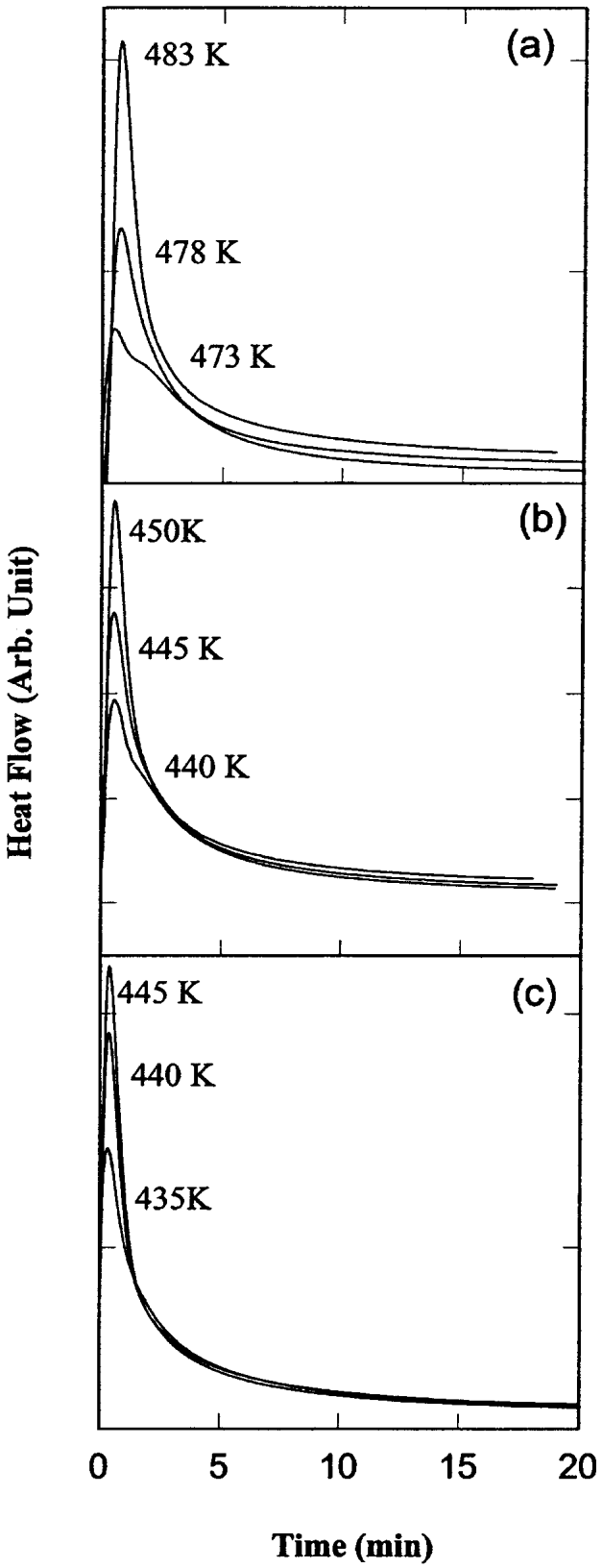

Fig. 3 DSC traces from amorphous (**a**) $Al_{85}Y_5Ni_{10}$, (**b**) $Al_{85}Y_4Ni_{10}Si_1$, and (**c**) $Al_{85}Y_5Ni_9Si_1$ alloys during isothermal annealing at temperatures about 5-15 K lower then their first crystallization peaks

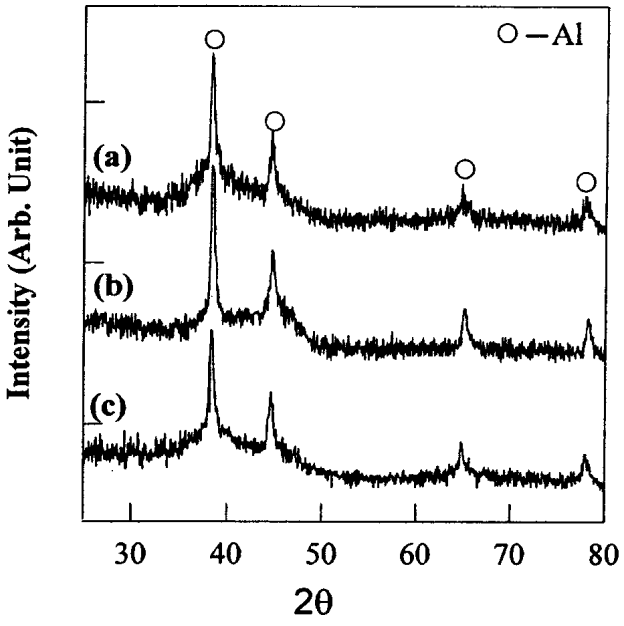

Fig. 4 XRD spectra from (**a**) $Al_{85}Y_5Ni_{10}$, (**b**) $Al_{85}Y_4Ni_{10}Si_1$, and (**c**) $Al_{85}Y_5Ni_9Si_1$ alloys after heating to the temperatures above the first crystallization peaks

Clearly, the growth of the particles is slower than predicted, however, this may be explained by considering soft impingement of the diffusion field between two particles. This description is also consistent with the model,[14] whereby as the Al particles crystallize, growth is limited by the diffusion of the rejected Y and Ni solute atoms. On the other hand, the growth process is also characterized by the small activation energy in the Al-based amorphous alloys. The activation energy was determined from the variation of the peak temperature with heating rate as determined by the Kissinger method.[15] The activation energies are about 200 kJ mol^{-1} and 250 kJ mol^{-1}, respectively, for the first crystallization peaks and second crystallization peaks. The activation energy for the growth of nanocrystal Al particles is very close to that for diffusion activation energy in $Fe_{40}Ni_{40}B_{20}$ (i.e., Q = 2.1 eV = 202 kJ mol^{-1}).[16] In contrast, the activation energy was about 242 kJ mol^{-1} (~2.52 eV) for the growth process of quasi-crystals in the amorphous phase and about 180 kJ mol^{-1} (~1.87 eV) for the transformation of quasi-crystals to the crystalline phase in Al-Mn films.[17] Therefore, it appears that the growth mechanism is dominated by different factors in different alloy systems. On the other hand, the measured values of the activation energy for the second exothermic peak were higher than that of the first exothermic peak, indicating a comparatively more stable amorphous matrix after the primary crystallization of the α-Al phase.

To determine the products of crystallization, the melt-spun ribbons were annealed at different temperatures, corresponding to the end temperatures of the first and the second exothermic reactions as shown in Fig. 2. Then the annealed samples were investigated using XRD. Figure 4 shows XRD spectra from $Al_{85}Y_5Ni_{10}$, $Al_{85}Y_4Ni_{10}Si_1$, and $Al_{85}Y_5Ni_9Si_1$ alloys after heating to the temperatures above the first crystallization peak. XRD traces consisted of an amorphous halo pattern and dif-

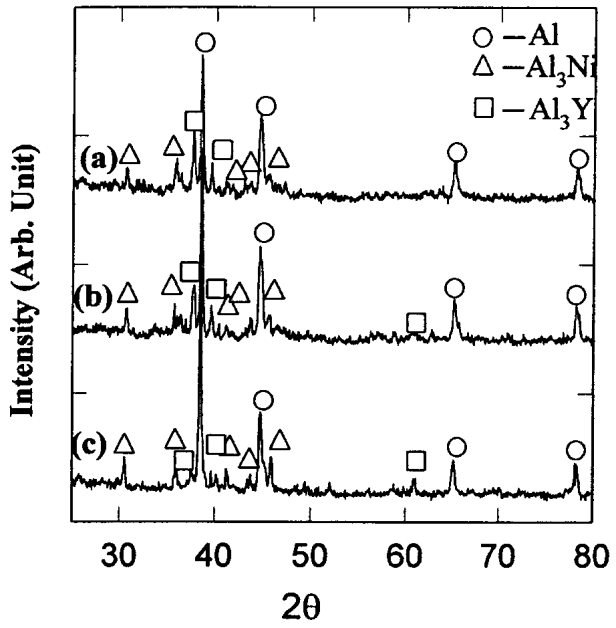

Fig. 5 XRD spectra from (**a**) $Al_{85}Y_5Ni_{10}$, (**b**) $Al_{85}Y_4Ni_{10}Si_1$, and (**c**) $Al_{85}Y_5Ni_9Si_1$ alloys after heating to the temperatures above the second crystallization peaks

fraction peaks from a crystalline phase. The diffraction peaks were analyzed as corresponding to a face-centered cubic solid solution with a lattice constant of 0.4055 nm, slightly larger than the lattice constant of pure Al. Thus, the XRD result revealed that for $Al_{85}Y_5Ni_{10}$, $Al_{85}Y_4Ni_{10}Si_1$, and $Al_{85}Y_5Ni_9Si_1$ alloys the first crystallization peak corresponded to the formation of α-Al nanocrystals in the amorphous matrix. This is in good agreement with previous results obtained by Gögebakan.[12] The size of the α-Al particles determined by using the broadening of XRD peaks was about 25 nm. Figure 5 shows XRD spectra from $Al_{85}Y_5Ni_{10}$, $Al_{85}Y_4Ni_{10}Si_1$, and $Al_{85}Y_5Ni_9Si_1$ alloys after heating to temperatures above the second crystallization peak. The XRD result revealed that for $Al_{85}Y_5Ni_{10}$, $Al_{85}Y_4Ni_{10}Si_1$, and $Al_{85}Y_5Ni_9Si_1$ alloys the second crystallization peak corresponded to the formation of a mixture of Al-rich intermetallic phases such as hexagonal Al_3Y with lattice constants of a = 6.192 Å and c = 21.125 Å, and orthorhombic Al_3Ni with lattice constants of a = 6.5796 Å, b = 7.352 Å, and c = 4.802 Å. This is again in good agreement with the previous study on the AlYNi alloy.[12]

Although no incubation stage was seen for the first exothermic peak of the $Al_{85}Y_5Ni_{10}$, $Al_{85}Y_4Ni_{10}Si_1$, and $Al_{85}Y_5Ni_9Si_1$ alloys, isothermal calorimetry experiments for the second exothermic peak showed a clear incubation period, followed by an exothermic peak. Then a rapid decrease in the reaction occurred, which is typical for a nucleation-and-growth mechanism. This is shown in Fig. 6. This suggests that the formation of intermetallic phases could be taking place by nucleation and growth since the existence of the incubation period indicates the presence of a thermally activated nucleation barrier. Interestingly, isothermal calorimetry traces of the $Al_{85}Y_5Ni_{10}$ alloy show two exothermic peaks corresponding to the second and third exothermic peaks from the continuous heating DSC trace

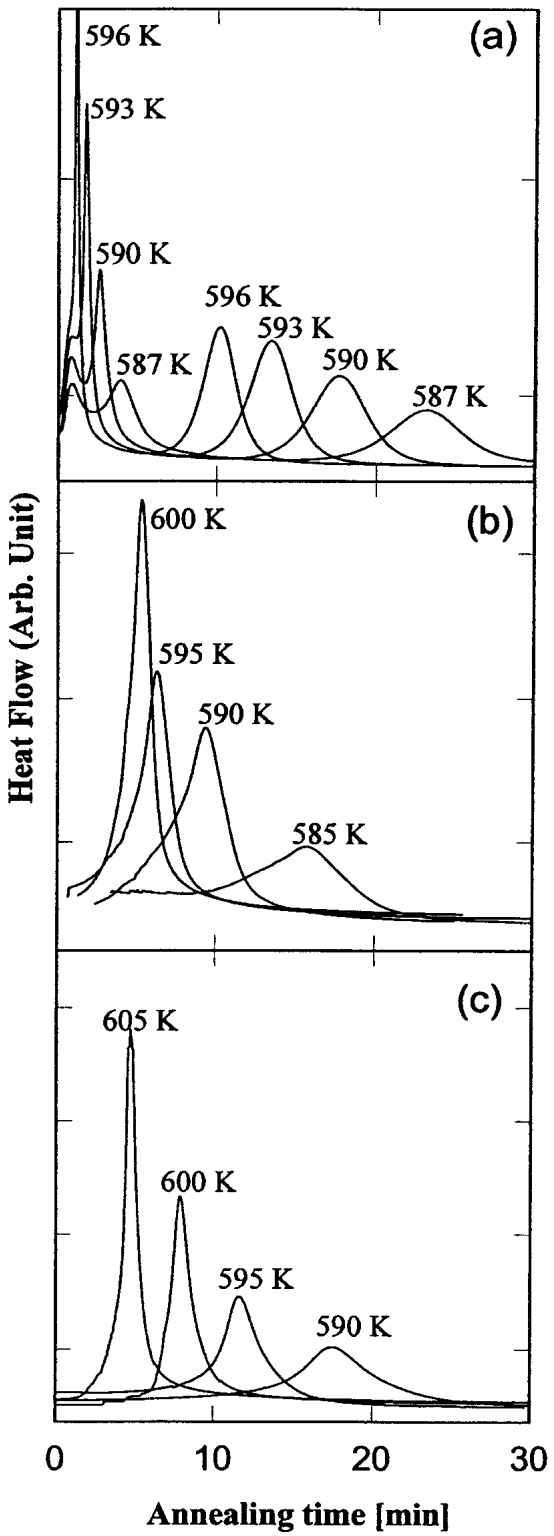

Fig. 6 DSC traces of amorphous (**a**) $Al_{85}Y_5Ni_{10}$, (**b**) $Al_{85}Y_4Ni_{10}Si_1$, and (**c**) $Al_{85}Y_5Ni_9Si_1$ alloys during isothermal annealing at temperatures about 5-15 K lower than their second crystallization peaks

in Fig. 2(a). Analyzing the isothermal curve using the JMA method gave Avrami time exponents in the range of 3.00-3.45. A high Avrami time exponent indicates that the crystallization

Table 1 Mechanical Properties of AlYNiSi Amorphous Ribbons

Alloys	σ_f, MPa	H_v, DPN
$Al_{85}Y_5Ni_{10}$	1050	380
$Al_{85}Y_4Ni_{10}Si_1$	1250	398
$Al_{85}Y_5Ni_9Si_1$	1230	390

process involved nucleation in addition to growth. Therefore, the simultaneous formation of two phases at a quite high Avrami exponent (i.e., 300-3.45) may correspond to interface-controlled growth by a eutectic reaction with a decreasing nucleation rate (assuming, of course, that the growth is three-dimensional).[13]

The tensile fracture strength (σ_f) and Vickers hardness (H_v) of $Al_{85}Y_5Ni_{10}$, $Al_{85}Y_4Ni_{10}Si_1$ and $Al_{85}Y_5Ni_9Si_1$ amorphous ribbons are summarized in Table 1. It can be seen from the Table 1 that these alloys have tensile strengths greater than 1000 MPa, with the highest σ_f value reaching 1250 MPa for the $Al_{85}Y_4Ni_{10}Si_1$ alloy. The tensile strengths of these amorphous alloys are about two to three times higher than the highest values[18] of commercial Al-based crystalline alloys. H_v values are about 390 diamond pyramid hardness number (DPH) (1 DPH = 1 kg/mm^2 = 9.8 MPa), which is twice as large as conventional Al-based crystalline alloys.[18] Therefore, we can say that the rapidly solidified $Al_{85}Y_5Ni_{10}$, $Al_{85}Y_4Ni_{10}Si_1$, and $Al_{85}Y_5Ni_9Si_1$ amorphous ribbons have very high tensile strengths, and very high H_v values. On the other hand, it appears that 1 at.% substitutions of Si for Y or Ni increase the mechanical properties of the amorphous ribbons. Therefore, the mechanical properties of these amorphous ribbons have improved by the addition of 1 at.% Si.

4. Conclusions

In the present research, the effect of Si additions on the crystallization behavior of amorphous $Al_{85}Y_5Ni_{10}$ has been investigated by replacing Y and Ni by 1 at.% Si. Continuous DSC traces from as-melt-spun ribbons consisted of three exothermic peaks and showed no glass transition prior to crystallization. Substitutions of Si for Y or Ni were found to decrease the thermal stability of the amorphous phase. The first exothermic peak for all alloys corresponded to the formation of α-Al phases. The second exothermic peak occurred at relatively high temperatures, and corresponded to the formation of intermetallic phases such as Al_3Ni and Al_3Y. Isothermal calorimetry traces for the first exothermic peak showed that the reaction occurred without any incubation period, and JMA analyses gave an Avrami time exponent between 1.00 and 1.16. This Avrami time exponent indicated that the transformation mechanism occurred by the diffusion-controlled growth of α-Al nanocrystals with soft impingement of the diffusion field between particles. Isothermal calorimetry traces for the second exothermic peaks showed that reactions occur with an incubation period. JMA analyses gave Avrami time exponent values between 3.00 and 3.45. These high Avrami values indicated that the transformation process takes place by a decreasing the nucleation rate with interface-controlled growth. σ_f and H_v values for AlYNiSi amorphous ribbons are in the range 1050-1250 MPa and 380-398 DPH, respectively, which is approximately twice as large as those for conventional Al-based crystalline alloys. Substitutions of Si for Y or Ni increased the mechanical properties of the amorphous ribbons.

Acknowledgments

I would like to thank Kahramanmaras Sutcu Imam for its financial support (Project No: 2003/2-10).

References

1. Y.H. Kim, K. Hiraga, A.Inoue, T. Masumoto, and H.H. Jo: "Crystallization and High Mechanical Strength of Al-Based Amorphous Alloys," *Mater. Trans. JIM* 1994, *35,* pp. 293-302.
2. Z.C. Zhong, X.Y. Jiang, and A.L. Greer: "Microstructure and Hardening of Al-Based Nanophase Composites," *Mater. Sci. Eng.*, 1997, *A226-228*, pp. 531-35.
3. Y.H. Kim, A. Inoue, and T. Masumoto: "Ultrahigh Tensile Strengths of $Al_{88}Y_2Ni_9M_1$ (M = Mn or Fe) Amorphous Alloys Containing Finely Dispersed fcc-Al Particles, *" Mater. Trans. JIM*, 1990**,** *31,* pp.747-49.
4. S.J. Hong, P.J. Warren, and B. S. Chun: "Nanocrystallization Behaviour of Al-Y-Ni with Cu Additions," *Mater. Sci. Eng. A*, 2001, *304-306*, pp. 362-66.
5. J. Latuch, A. Kokoszkiewicz, and H. Matyja: " The Effect of Cu Addition on the Formation of fcc-Al Phase in Rapidly Quenched Al-Y-Ni Alloys," *Mater. Sci. Eng. A*, 1997, *226-228*, pp. 809-12.
6. N. Bassim, C.S. Kiminami, M.J. Kaufman, M.F. Oliveira, M.N.R.V. Perdigao, and W.J. Botta Filho: "Crystallization Behaviour of Amorphous $Al_{84}Y_9Ni_5Co_2$ Alloy," *Mater. Sci. Eng. A,* 2001, *304-306,* pp. 332-37.
7. T.S. Kim, S.J. Hong, J.H. Lee, and K.W. Kim, "Structural Change of the Melt Spun Al-10Ni-5Y by the Addition of 1% Sr," *Mater. Sci. Eng.. A,* 2001, *311*, pp. 226-31.
8. M. Yewondwossen, R.A. Dunlapand, and D.J. Lloyd: "Thermal and Electronic Properties of Amorphous $Al_{87}Y_8Ni_{5-x}TM_x$ (TM = Mn, Fe, Co. Cu)," *J. Phys. Condens. Matter*, 1992, *4,* pp. 461-72.
9. B.D. Cullity and S.R. Stock: *Elements of X-Ray Diffraction*, 3rd ed., Prentice-Hall, Inc., Englewood Cliffs, NJ, 2001.
10. A. Inoue: "Amorphous, Nanoquasicrystalline And Nanocrystalline Alloys in Al-Based Systems," *Prog. Mater .Sci*, 1998, *43,* pp. 365-520.
11. A. Inoue, K. Nakazato, Y. Kawamura, A. P.Tsai, and T. Masumoto: "Effect of Cu or Ag on the Formation of Coexistent Nanoscale Al Particles in Al-Ni- M-Ce (M = Cu or Ag) Amorphous Aloys," *Mater. Trans. JIM,* 1994, 35, pp. 95-102.
12. M. Gögebakan: "Amorphous and Nanocrystalline Al-Based Alloys," Ph.D. Thesis, University of Oxford, Oxford, UK, 1998.
13. J.W. Christian: *Theory of Transformation in Metals and Alloys*, Pergamon Press, Oxford, UK, 1975.
14. A.P. Tsai, T. Kamiyama, Y. Kawamura, A. Inoue, and T. Masumoto: "Formation and Precipitation Mechanism of Nanoscale Al Particles in Al-Ni Base Amorphous Alloys," *Acta Metall. Mater.*, 1997*, 45,* pp. 1477-87.
15. H.E. Kissinger: "Reaction Kinetics in Differential Thermal Analysis," *Anal. Chem.*, 1957, *29*, pp. 1702-06.
16. B. Cantor and R.W. Cahn: *Amorphous Metallic Alloys*, F.E. Luborsky, ed., Butterworth Heinemann, Burlington, MA, 1983.
17. L.C. Chen, F. Spaepen, J.L. Robertson, S. C. Moss, and K. Hiraga: "A Structural and Calorimetric Study of the Transformations in Sputtered Al-Mn and Al-Mn-Si films," *J. Mater. Res.,* 1990, *5,* pp. 1871-79.
18. Anon.: *Metals Databook*, Japan Institute of Metals, Tokyo, Japan, 1983.